Journal of Engg. Research Vol. 8 No. (1) March 2020 pp. 211-230

A new fluctuating power decoupling method based on ANFIS and PR control structures applicable to single-phase PWM rectifiers

H. Rezaie*, A. Khoshsaadat**, J. S. Moghani* and H. Rastegar*

**Department of Electrical Engineering, Amirkabir University of Technology, Tehran, Iran*
***Department of Electrical Engineering, Ayatollah Boroujerdi University, Borujerd, Iran*
**Corresponding Author: h.rezaie@aut.ac.ir*

ABSTRACT

In the input power of single-phase rectifiers, there is a pulsating portion with twice the grid frequency. To prevent the transferring of the pulsating power to the DC side, it should be filtered appropriately. For this purpose, a convenient method is to install a high-capacitance capacitor at the DC side, which cannot be considered as a proper solution due to its undesirable characteristics. This paper proposes an active method to eliminate the pulsating power, in which the control system is based on Adaptive Network-based Fuzzy Inference System (ANFIS) architecture. To improve the controller performance, an online supervisory learning algorithm based on the Error Back Propagation (EBP) learning method is employed. This technique leads to the forming of a control system with minimal structure, enhanced accuracy, and improved dynamics. Also, the proposed control strategy is implemented using a Proportional Resonant (PR) compensator, and the performances of two controllers are compared with each other and with one of the most outstanding previous works as well. Moreover, a superseded control method based on ANFIS architecture for the conventional control system of single-phase PWM rectifiers is suggested. The efficiency of the proposed methods is confirmed by extensive simulations in MATLAB/Simulink.

Keywords: Single phase PWM rectifier; pulsating power; active power decoupling; ANFIS controller; fuzzy control; auxiliary energy storage.

INTRODUCTION

Single-phase Pulse Width Modulation (PWM) rectifier has several residential and industrial applications such as DC power supplies, Uninterruptible Power Supplies (UPSs), and AC-fed railway traction drives. These rectifiers can provide current with low harmonic distortions, and the unity power factor operation. However, one of their main problems is a pulsating power with twice the grid frequency at the AC side; if the pulsating power is not effectively eliminated, it will be transferred to the DC-Link and affect the DC loads' performance. For example, when a battery is used as the DC load, the pulsating power causes overheating and decreasing lifetime of the battery, or in the inverter-mode of the converter, it has unpleasant effects on the Maximum Power Point Tracking (MPPT) performance of grid-connected single-phase photovoltaic systems (Shimizu et al., 1997, & Tang et al., 2015).

A conventional method to filter the pulsating power is to install a large DC-link capacitor. Usually, the appropriate capacitor for this purpose is a short lifetime and large size electrolytic capacitor, such as Aluminum Electrolytic (AE) capacitor, which reduces the power density and reliability of the converter (Wang et al., 2011). So far, to solve this problem, several active power decoupling methods have been suggested, in which the basic idea is transferring the alternative section of the power to an auxiliary energy storage element (inductor or capacitor). Thereby, a small capacitor with a long lifetime, such as film capacitor, can be used as the output filter instead of a large capacitor, reduce the size and cost, and also increase the reliability of the converter (Su et al., 2014). In the active power decoupling methods, the pulsating power can be transferred to the auxiliary energy storage element by two different techniques:

1) By adding active elements (switches) to the rectifier circuit; for example, a third-leg can be added to the main rectifier circuit for transferring the pulsating power to the auxiliary energy storage element. The advantage of this case is that the rectifier's main controller can remain unchanged and the rectifier can work properly with/without the active power decoupling circuit.

2) Without adding active elements to the rectifier circuit; e.g., the auxiliary energy storage element can be placed between the second-leg of the main circuit of the rectifier and the output filter, and by modifying the control system of the rectifier, the second-leg can conduct the pulsating power to the energy storage element. The advantage of this method is that the number of additional components is reduced. However, these methods usually have more complexity in the control system and less flexibility in the modulation and controller design.

In the following, some of the active methods introduced in the previous works are mentioned. In (Wang et al., 2011 & Li et al., 2013), a third-leg (including two switches and two reverse-parallel diodes) is added to the main circuit, which transfers the alternative power to the auxiliary energy storage element. In Su et al. (2014), a similar structure is used, but the difference is that the additional leg has only one switch and one diode. As a merit of this work, the number of elements is reduced, but the control system has become more complicated because the reference current for the power decoupling is a rectified sinusoidal signal. Elimination of the pulsating power has been achieved by a buck-boost converter that is placed between the rectifier circuit and the output capacitive filter in Zhong et al. (2012). Unlike the other mentioned works, in Tang et al. (2015), a diode bridge is used as the rectifier and the fluctuating power is absorbed by a half-bridge converter. In Tang & Blaabjerg (2015) and Qi et al. (2014), transferring the pulsating power to the auxiliary energy storage element is realized without any additional active elements. In these methods, the alternative power is filtered by changing the conventional control system and proper placement of the auxiliary energy storage elements. It should be noted that the auxiliary energy storage can be inductive or capacitive. As a comparison between them, although capacitors have higher power density and lower power losses, inductors are more reliable and robust (Tang et al., 2015).

In this paper, a new control approach based on Adaptive Network-based Fuzzy Inference System (ANFIS) and Proportional Resonant (PR) control structures for active power decoupling is proposed. Due to the advantages of the inductive filters, in the proposed method, an inductive auxiliary energy storage is used. Also, in the proposed control method, the current of the auxiliary inductor has a sinusoidal reference signal that makes its tracking simpler than non-sinusoidal signals, which have been chosen as the reference signal in some other papers. Moreover, in this paper, to transfer the fluctuating power to the auxiliary energy storage element, the mentioned method "1" is applied; it means that the proposed method does not need to change the conventional PWM control method of the single-phase rectifier, so the rectifier will have an appropriate performance with/without the power decoupling circuit. The basic structure of the control system proposed in this work is simpler than other previous methods and the ANFIS controller is designed in such a way that it has the least possible amount of calculations.

In this paper, the ANFIS controller is used for utilization of parallel processing, learning, and adaptation abilities of Neural Network (NN) and inference capability of Fuzzy Logic (FL), simultaneously. The controller is adaptive with variation in the system conditions and has minimum fuzzy rules for inference engine that provides a control system that requires the minimum amount of calculations. The obtained results demonstrate that the suggested controller is able to track the reference signal with adequate correctness and very fast transient. This controller is based on the IF-THEN rules of fuzzy logic, which are based on an ordinary engineering knowledge about the converter performance. To train the suggested controller, one approach of the Error Back Propagation (EBP) learning method is used with the minimum amount of calculations. The architecture of ANFIS is a five-layer NN with 6-9-9-9-1 nodes to implement the five parts of the ANFIS controller. The efficiency of the suggested controller is investigated by system simulation in various situations.

In the following of this paper, first, single-phase PWM AC/DC converters are studied and the basis of the suggested method to eliminate the pulsating power is described. Then, the proposed control technique is presented, and the design and performance of PR and ANFIS controllers are discussed. Finally, the effectiveness of the superseded

control method for single-phase PWM rectifiers and the proposed methods for the power decoupling are verified by system simulation in various conditions. Also, the results obtained in simulations are compared with those of another paper, in the simulation results section.

SINGLE-PHASE PWM RECTIFIER WITH PULSATING POWER DECOUPLING CAPABILITY

Figure 1 presents a typical topology of a single-phase PWM rectifier. Suppose the voltage of the AC source is as (1).

$$v_S(t)=V_S\sin(\omega t) \tag{1}$$

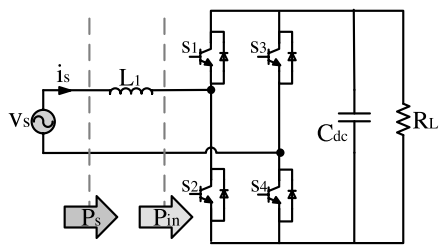

Figure 1. A typical topology of a single-phase PWM rectifier.

By assuming operating at the unity power factor, the source current should be as follows:

$$i_S(t)=I_S\sin(\omega t) \tag{2}$$

The input power can be obtained from (3).

$$P_S=v_S(t)i_S(t)=\frac{V_SI_S}{2}-\frac{V_SI_S}{2}\cos(2\omega t) \tag{3}$$

By multiplying the current and voltage of L_1, its instantaneous power can be calculated as

$$P_{L_1}=L_1\frac{di_S}{dt}\times i_S=\frac{1}{2}L_1I_S^2\omega\sin(2\omega t) \tag{4}$$

So, the input power of the rectifier can be obtained by (5).

$$P_{in}=P_S-P_{L_1} \tag{5}$$

By substituting (3) and (4) in (5), (6) will be achieved.

$$P_{in}=\frac{V_SI_S}{2}-\frac{V_SI_S}{2}\cos(2\omega t)-\frac{1}{2}L_1I_S^2\omega\sin(2\omega t)=P_{const.}+P_r \tag{6}$$

where ω is the angular frequency of the AC source, and I_S and V_S represent the amplitude of the input current and voltage, respectively.

According to (6), there is a pulsating section with twice the grid frequency in the input power of rectifier, which should be eliminated effectively. In this work, to diminish the capacitance required for the output filter, the alternative power is absorbed by an auxiliary inductor. Figure 2 represents the proposed topology; it is composed

of the single-phase PWM rectifier and an additional leg that conducts the pulsating power to the auxiliary energy storage element (L_f). It should be noted that the used topology in this work has already been used in Shimizu et al. (2000), but the structure of the control systems is utterly different. In Shimizu et al. (2000), the current of the inductor is controlled based on the sensing the ripple of the output current, and it has a complicated controller. But, in the proposed method, the reference current of the auxiliary inductor is calculated based on the power decoupling calculation. The proposed control method requires less amount of calculations and also is designed based on a simpler concept in comparison to the method employed in Shimizu et al. (2000).

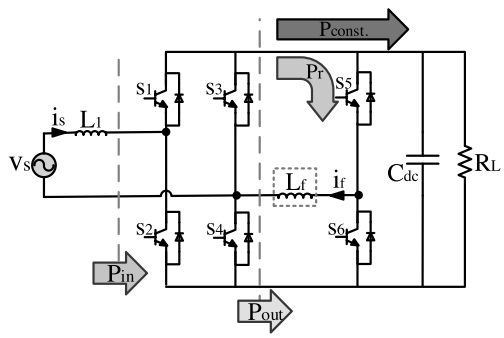

Figure 2. The topology used in the proposed pulsating power elimination method.

By neglecting the converter loss, the rectifier output and input power are equal. Therefore, to attain a successful power decoupling, the fluctuating part of the power should be absorbed by L_f and the constant part should feed the load. Hence,

$$P_r = P_{L_f} \tag{7}$$

According to (6), and by using trigonometric equations, P_r can be rewritten as follows:

$$P_r = -\frac{1}{2}\sqrt{\left(L_1 I_S^2 \omega\right)^2 + \left(V_S I_S\right)^2}\sin(2\omega t+\alpha) \tag{8}$$

where $\alpha = \tan^{-1}(V_S / L_1 \omega I_S)$. Due to the fact that P_r pulsates at twice of the grid frequency and it must be equal to the power of L_f, the reference current of L_f must have a sinusoidal waveform with the grid frequency. So, the current of the auxiliary inductor should be as

$$i_f(t) = I_f \sin(\omega t+\theta) \tag{9}$$

So, the power of L_f can be expressed by

$$P_{L_f} = L_f \frac{di_f}{dt} \times i_f = \frac{1}{2} L_f I_f^2 \omega \sin(2\omega t+2\theta) \tag{10}$$

According to (7),

$$-\frac{1}{2}\sqrt{\left(L_1 I_S^2 \omega\right)^2 + \left(V_S I_S\right)^2}\sin(2\omega t+\alpha) = \frac{1}{2} L_f I_f^2 \omega \sin(2\omega t+2\theta) \tag{11}$$

That can be rewritten as follows:

$$\sqrt{\left(L_1 I_S^2 \omega\right)^2 + \left(V_S I_S\right)^2}\sin(2\omega t+\alpha) = L_f I_f^2 \omega \sin(2\omega t+2\theta+\pi) \tag{12}$$

From the above equation, the current amplitude of L_f and the phase difference between i_f and the source voltage (θ) can be calculated as follows:

$$I_f = \sqrt[4]{\frac{\left(V_S I_S\right)^2 + \left(L_l \omega I_S^2\right)^2}{\left(L_f \omega\right)^2}} \quad (13)$$

$$\theta = \frac{\alpha - \pi}{2} \quad (14)$$

The reference current of L_f (i_f^*), to suppress the fluctuating power, can be obtained by substituting (13) and (14) into (9). Considering the aforementioned explanations, by using an appropriate controller, which is able to control the current of L_f according to its calculated reference (i_f^*), the auxiliary inductor (L_f) can absorb the fluctuating power effectively. Hence, there will be almost no second-order harmonic at the output voltage, and the DC-link capacitor should just filter the higher-order harmonics that leads to significantly diminishing its required capacitance. It allows the use of a small capacitor with a long lifetime as the output filter instead of a large capacitor with a short lifetime and large size.

CONTROLLER DESIGN

In the proposed control strategy, transferring the alternative power to the auxiliary energy storage element is performed through the mentioned method "1" in "INTRODUCTION". In this method, there is no need to change the conventional PWM control method of the single-phase rectifier, and it has a suitable performance with/without the power decoupling circuit.

A suitable rectifier has three characteristics: 1) adjusting the output voltage according to its reference with the minimum of oscillations, 2) providing an input current with the minimum of harmonic distortions, and 3) being able to operate at the unity power factor.

The conventional controller of the single-phase PWM rectifier is presented in Figure 3, part i, which is composed of two portions (Rezaei et al., 2015):

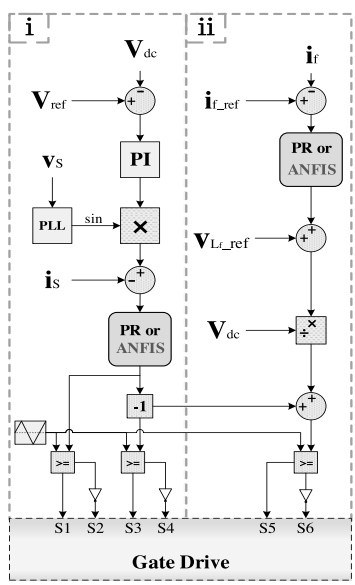

Figure 3. The schematic diagram of the control system.

a) Voltage control outer-loop: In this part, the DC voltage error is given to a PI controller to get a quick response with zero steady state error. By multiplying the output of the PI controller and a unit amplitude sinusoidal waveform, which is synchronized with the source voltage, the reference input current is achieved. Synchronizing the reference current with the source voltage provides the unity power factor operation. To generate a synchronized signal with the source voltage, a Phase-Locked Loop (PLL) is used; a PLL is a closed-loop system, which provides an output signal synchronized in phase and frequency with its input signal (Rezaie et al., 2016).

b) Current control inner-loop: The function of this part is controlling the input current according to the reference signal and generating the modulation signal. In the conventional control method of single-phase PWM rectifier, to regulate the input current, a PR controller is used. In this work, a new controller based on ANFIS architecture is suggested for this purpose. In "ANFIS controller" section, the ANFIS controller design is expressed in detail. In the simulation results section, by comparing the results obtained by two controllers, the effectiveness of the suggested superseded controller is confirmed.

In the control system, the unipolar switching pattern is employed for two reasons:

1) reducing the output voltage ripple and 2) increasing the effective switching frequency (Mohan & Undeland, 2007).

Figure 3, part ii, represents the controller of the third-leg that conducts the fluctuating power into L_f. Because the reference current in the proposed method is a sinusoidal waveform, its regulation can be appropriately performed by using a PR controller that provides a simpler controller compared to other techniques, which have a non-sinusoidal reference signal for the voltage or the current of the auxiliary energy storage element. In the next part, the PR controller is explained, and its performance is analyzed by bode diagrams. Moreover, in this paper, the ANFIS controller is used instead of the PR controller in the proposed method. In the simulation results section, the effectiveness of both proposed control methods is confirmed by extensive simulations; also two controllers have been compared with each other in different aspects. After current regulation, for determining the switching pattern of the additional leg, a relation between the main circuit of the rectifier and the switches of the third-leg must be established. Due to the relatively high switching frequency, the converter averaged model can be utilized, and the relation can be appointed simply according to (15) (Yazdani & Iravani, 2010).

$$V_{L_f} = (d_c - d_b)V_{dc} \tag{15}$$

That leads to the following equation:

$$d_c = \frac{V_{L_f}}{V_{dc}} + d_b \tag{16}$$

where V_{Lf} is the average voltage between the second and third leg (the voltage across the auxiliary inductor L_f) during one switching cycle, and d_c and d_b represent the duty ratio of S5 and S3, respectively. In Figure 3, part ii, the control structure to generate the modulating signal for the switching of the third-leg is implemented based on (16).

PR controller

The PI controller ($G_{PI}(S)=k_P+k_I/S$) provides an infinite gain at $\omega=0$ and a quick response to a DC reference with zero steady state error. The PR controller performance is almost similar to a PI controller, but the difference is that this controller can correctly track an AC reference waveform, because it can provide an infinite gain at an arbitrary frequency, called resonant frequency, with zero phase shift and nearly no gain in other frequencies (Zhang et al., 2014). The ideal transfer function for a PR compensator is defined as

$$G_{PR}(S) = k_P + \frac{2k_r S}{S^2 + \omega^2} \tag{17}$$

where k_P is the proportional gain, k_r is the integral gain, and ω is the resonant frequency. The bode diagram of the ideal PR compensator is presented in Fig. 4(a). Due to the infinite gain, the ideal PR compensator is faced with the stability problem. In addition, it has a high sensitivity to the frequency variations. Therefore, it cannot be implemented in practice. The non-ideal PR controller transfer function is expressed in equation (18), which can be a proper practical alternative for the ideal PR controller.

$$G_{PR}(S)=k_P+\frac{2k_r\omega_C S}{S^2+2\omega_C S+\omega^2} \tag{18}$$

where ω_C is the bandwidth around the resonant frequency that reduces the sensitivity against the frequency variations. Although the gain at the resonant frequency is finite, it is still sufficiently high to obtain a very small steady state error. Fig. 4(b) represents the bode diagram of a non-ideal PR compensator in which k_p specifies the controller dynamics, bandwidth, phase, and gain margins, and k_r specifies the amplitude gain at the resonant frequency and adjusts the bandwidth around it (Zammit et al., 2014). Figure 5 presents the amplitude and phase variations of the PR controller for different values of k_p and k_r.

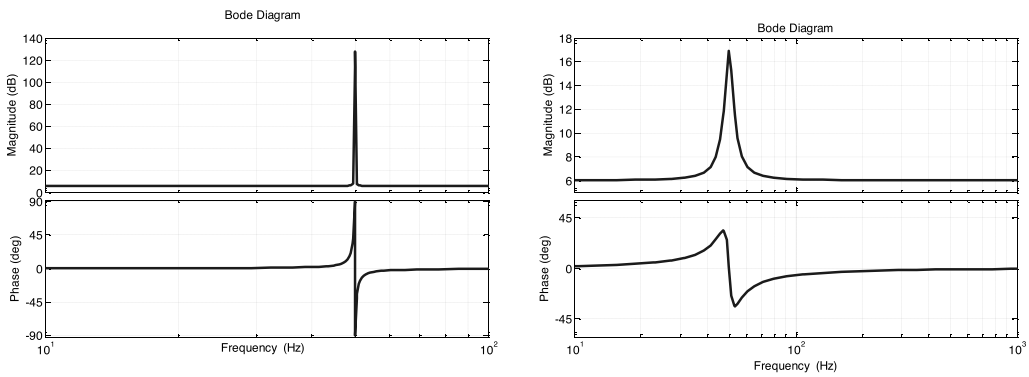

(a) (b)

Figure 4. Bode diagram of the PR controller; k_p=2, k_r=5 and ω=314(rad/S) (a) ideal (b) non-ideal; ω_C =10(rad/S).

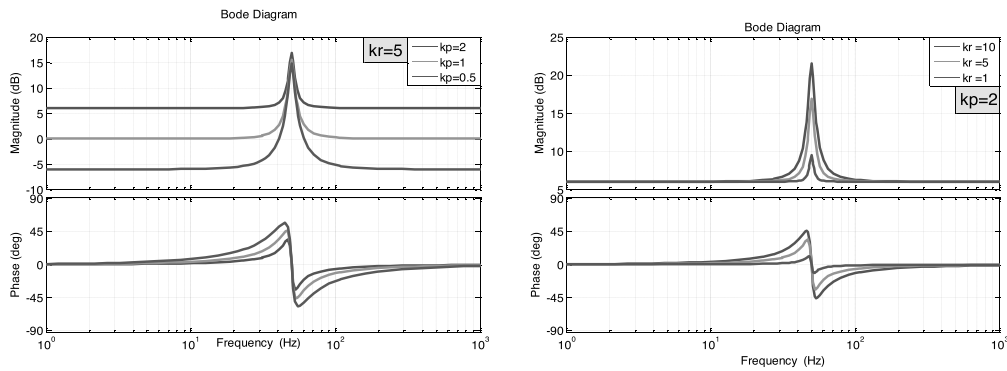

(a) (b)

Figure 5. The amplitude and phase changes of the PR controller; ω_C =10(rad/S) and ω=314(rad/S) (a) for different values of k_p (b) for different values of k_r.

ANFIS controller

In the ANFIS architecture, the control system is established based on a set of fuzzy rules that receives crisp inputs and after mapping them to the fuzzy area, it processes the data according to the inference rules and finally gives the output. These processes are implemented using a five-layer NN, for using the parallel processing and the learning ability of the NN besides the inference ability of the FL (Tripura & Babu, 2014).

The 'IF X_1 is α & X_2 is β, THEN Y is γ' rule-base as a look-up-table is applied to describe the expert's knowledge for implementation of the FL system. In Figure 6, the triangular membership functions of the inputs used in this work are shown. This type of function has a minimum mass of calculation compared to other membership functions such as bell-shaped or Gaussian functions. The basic concept of FL is the use of a look-up-table of the two fuzzy inputs and computes the output from fuzzy operating on them. To design the controller, the current error and its time derivative (shown with e and de, respectively) are considered as two inputs of the FL system. The scale of each of the two fuzzified inputs is divided to three fuzzy confines. Considering these two inputs and their scaling, the output will have 9 arrays. In Figure 6, the membership functions of the input variables used in this work are shown with the three sets Negative (NE), Zero (ZE), and Positive (PO) as fuzzy measures. Finally, the database includes 9 rules as the inference engine, which is represented in Table 1. Although the fuzzy rules could be more, for avoiding a large amount of processing, the minimum number of the fuzzy rules has been used in this controller (Rezaie et al., 2017).

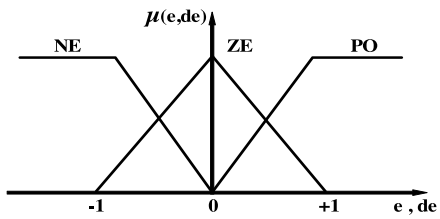

Figure 6. Membership functions for the two inputs of the ANFIS controller (the current error and its time derivative).

Table 1. Fuzzy rule base of the ANFIS controller.

Fuzzy Rules		de		
		NE	ZE	PO
e	PO	ZE	PS	PB
	ZE	NS	ZE	PS
	NE	NB	NS	ZE

It should be mentioned that, for implementing the proposed controller in practice, since the second input (time derivative of the current error) of the ANFIS controller is sensitive against noise, it is better to put a filter on the measured signals to enhance the system robustness and stability. For this application, usually, a simple first-order low-pass filter can properly work.

Fuzzy controllers are non-linear controllers, but they cannot be adjusted with variable situations. Furthermore, these types of controllers lack parallelism ability of the controllers designed based on NN (Liu & Tong, 2015). Also, NN is much more adaptive to different situations by accordingly adjusting its weights using the back-propagation of the errors to the hidden layers of the networks. To gain the benefits of the FL and NN simultaneously, and to overcome their deficiencies, a mixed system formed by their combination can be employed. Therefore, in the second phase of the scheme, the NN for implementation of the FL system is used. One of the most popular methods for this combination is the use of the ANFIS architecture that is one of the types of hybrid neuro-fuzzy systems. Figure 7 presents the structure of the suggested ANFIS controller, which is employed as a current controller. In this case, the current error and its time derivative are used as the inputs of the NN.

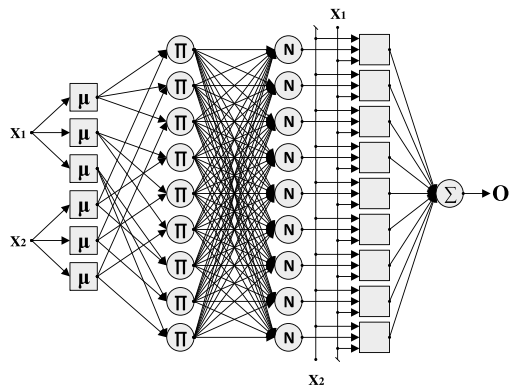

Figure 7. The structure of the proposed ANFIS controller.

According to Figure 7, the architecture of the NN consists of five layers (Masood et al., 2012);

Layer 1: Each node of this layer produces a membership grade of one of the linguistic labels. Also, this layer confines the area of each crisp input to one fuzzy area. The membership relation between the input and output of each node in this layer can be expressed as follows:

$$O_j^1=\begin{cases}\mu\left(X_1^1\right) & j=1,2,3\\ \mu\left(X_2^1\right) & j=4,5,6\end{cases} \tag{19}$$

where j is the number of neurons in this layer, and μ in the triangular membership function can be obtained by

$$\mu(X)=\begin{cases}0 & x\le a\\ \dfrac{x-a}{b-a} & a\le x\le b\\ \dfrac{c-x}{c-b} & b\le x\le c\\ 0 & c\le x\end{cases} \tag{20}$$

By using min and max, an alternative expression for (20) can be written:

$$\mu(X)=\max\left[\min\left(\frac{x-a}{b-a},\frac{c-x}{c-b}\right),0\right] \tag{21}$$

where a, b, and c are the membership function parameters, governing the triangular membership function accordingly. These parameters have been named as premise parameters of the ANFIS.

Layer 2: Each node of this layer has an output known as ‘’firing strength’’ of each rule of FL system via fuzzy multiplication principle:

$$O_j^2=\mu\left(X_1^2\right)\mu\left(X_2^2\right);\quad j=1,2,...,9 \tag{22}$$

Layer 3: This layer calculates the ratio of the strength of each rule to the sum of the strengths of all rules as follows:

$$O_j^3=\overline{W_j}=\frac{W_j}{\sum_{k=1}^{9}W_k};\quad j=1,2,...,9 \tag{23}$$

Layer 4: Each node of this layer has a node function as given in (24).

$$O_j^4=\overline{W_j}f_j=\overline{W_j}\left(p_jX_1+q_jX_2+r_j\right);\quad j=1,2,...,9 \tag{24}$$

where p_j, q_j and r_j are called consequent parameters of the ANFIS.

Layer 5: Finally, in this layer, one neuron exists that computes the overall summation of the incoming signals as

$$O_1^5=\sum_{k=1}^{9}\overline{W_k}f_k \tag{25}$$

In the suggested controller in this work, this node is single because the controller has one output.

Learning in ANFIS

In the ANFIS architecture, the rules are defined based on the Sugeno fuzzy model as follows:

IF X_i is A_i and Y_i is B_i, THEN $f_k=p_kX_i+q_kY_i+r_k$

One of the learning algorithms to update the ANFIS parameters is based on the hybrid-learning algorithm in which the consequent and premise parameters will be updated after each data presented to the algorithm, called Forward Signal and Backward Error Back-Propagation (FSBEBP). For training the network, there are two procedures: forward-pass and backward-pass; the forward-pass propagates the input vector through the network, layer by layer, and the consequent parameters are updated using the least squares estimate method. In the backward-pass, the error is sent back through the network in a similar manner to EBP. Indeed, in the backward-pass, the calculated errors will be passed back, and the premise parameters will be adjusted by the gradient descent technique.

For the ANFIS, the partial derivatives of the error function with respect to the fuzzy system parameters, which need to be tuned, must be attained. In other words, for each parameter g_i, (26) should be calculated:

$$\frac{\partial E_k}{\partial g_i}=\delta\frac{\partial E_k}{\partial O_k}\frac{\partial O_k}{\partial g_i}=\delta\left(O_k-y_k\right)\frac{\partial O_k}{\partial g_i} \tag{26}$$

where δ is the learning rate of the NN, O_k is the output of the k-th layer, and g_i is the ANFIS parameter that includes both the consequent and premise parameters. E_k is the cost function of the error and usually can be written as

$$E_k=\frac{1}{2}\left(d_k-O_k\right)^2 \tag{27}$$

where d_k is the desired response of the k-th layer, and O_k is the output of the k-th layer. The error rate for consequence parameters, using the chain law, can be calculated as follows:

$$\frac{\partial E_k}{\partial g_C}=\frac{\partial E_k}{\partial O_5}\frac{\partial O_5}{\partial O_4}\frac{\partial O_4}{\partial g_C} \tag{28}$$

which gives

$$\frac{\partial E_k}{\partial g_C}=\delta\left(O_5-d_5\right)\frac{\partial O_4}{\partial g_C} \tag{29}$$

That $\frac{\partial O_4}{\partial g_C}$ for three parameters of the THEN-part of the Sugeno rules can be written as

$$\frac{\partial O_4}{\partial p_k}=\overline{W_k}X,\quad \frac{\partial O_4}{\partial q_k}=\overline{W_k}Y,\quad \frac{\partial O_4}{\partial r_k}=\overline{W_k}; \tag{30}$$

where k is the proposed rule. For updating the premise parameters, using of the chain law, (31) can be written:

$$\frac{\partial E_k}{\partial g_p}=\delta\frac{\partial E_k}{\partial O_5}\frac{\partial O_5}{\partial O_4}\frac{\partial O_4}{\partial O_3}\frac{\partial O_3}{\partial O_2}\frac{\partial O_2}{\partial O_1}\frac{\partial O_1}{\partial g_p} \tag{31}$$

where g_p is the premise parameter. Calculation of each part of this equation will result in (32):

$$\frac{\partial E_k}{\partial g_p}=\delta\left(O_5-d_5\right)f_k\frac{\left(\sum_{j=1}^{9}w_j-w_i\right)}{\left(\sum_{j=1}^{9}w_j\right)^2}\frac{\partial\left(\prod_{k=1,k^1m}^{9}T_k\right)}{\partial T_m}\frac{\partial O_1}{\partial g_p} \tag{32}$$

where $\frac{\partial O_1}{\partial g_p}$ is the derivative of the output of the 1-th layer (triangular function) to the three parameters of the triangular membership function (a, b, and c). Notice that, for any of these three parameters, $\frac{\partial O_1}{\partial g_p}$ can be achieved as follows:

$$\text{For}\quad g_p=a;\quad \frac{\partial E_k}{\partial a}=\begin{cases}\dfrac{x-b}{(b-a)^2} & a\le x\le b\\ 0 & \text{otherwise}\end{cases} \tag{33}$$

$$\text{For}\quad g_p=b;\quad \frac{\partial E_k}{\partial b}=\begin{cases}\dfrac{a-x}{(b-a)^2} & a\le x\le b\\ \dfrac{c-x}{(c-b)^2} & b\le x\le c\\ 0 & \text{otherwise}\end{cases} \tag{34}$$

$$\text{For}\quad g_p=c;\quad \frac{\partial E_k}{\partial c}=\begin{cases}\dfrac{x-b}{(c-b)^2} & b\le x\le c\\ 0 & \text{otherwise}\end{cases} \tag{35}$$

SIMULATION RESULTS

To investigate the advantages of the suggested methods in the operation of the single-phase PWM AC/DC converter, diverse simulations have been done in MATLAB/Simulink. The solver used in the simulations was ode23tb with 1μs step size. Table 2 presents the parameters' value used in the simulation.

Table 2. The parameters used in the simulating the PWM rectifier.

System parameters	Source voltage	Grid frequency	Input inductance	Small/large DC-link capacitance	DC bus voltage	Output power	Switching frequency
variable	V_S	f	L_1	C_{dc}	V_{dc}	P_O	f_{sw}
value	220 V_{rms}	50 Hz	7 mH	220μF/2200 μF	450 V	4 kW	3 kHz

Simulation of the rectifier without the power decoupling circuit

First, the efficiency of the ANFIS controller instead of the PR controller in the conventional control system of the rectifier has been evaluated. Figures 8 and 9 show the DC-link voltage of the rectifier using the PR and ANFIS controllers. The used DC-link capacitor (C_{dc}) in Figure 8 and Figure 9 is 220 μF and 2200 μF, respectively. It is clear that the ANFIS controller performance in transient response is as well as the PR controller and has less overshoot compared to the PR controller. Another important aspect is the sensitivity of the PR controller against the variations in the values of system elements. The PR controller parameters are tuned according to the nominal and initial values of the system elements that will not remain constant over time and under different conditions. This challenge reduces the performance quality of the PR controller. But, because of online learning ability, the ANFIS controller is able to adapt itself to different situations. Hence, the ANFIS controller is more robust against the variations of system conditions, and it has lower sensitivity to the variations of elements values.

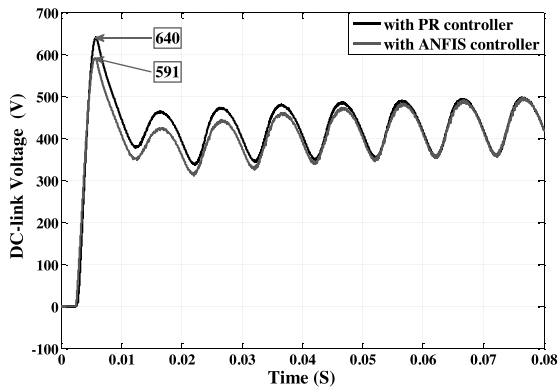

Figure 8. The DC-link voltage with the small capacitor using PR and ANFIS controllers.

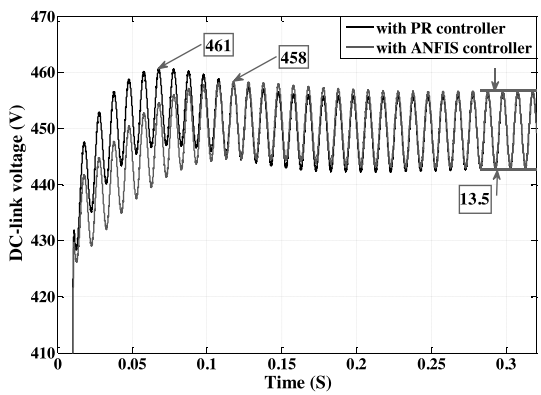

Figure 9. The DC-link voltage with the large capacitor using PR and ANFIS controllers.

Figure 10 represents the input current and voltage of the rectifier with the large DC-link capacitance (2200μF), using PR and ANFIS controllers. According to Figure 10, both controllers have desirable performance in synchronizing the input current with the input voltage and can provide the unity power factor operation.

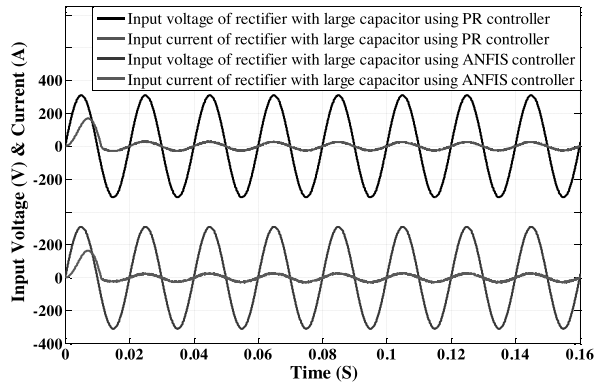

Figure 10. The input voltage and current with the large DC-link capacitor using PR and ANFIS controllers.

By using Simulink Fast Fourier Transform (FFT) analysis, the input current THD from 0.1 sec. to 0.6 sec. (25cycles) for PR and ANFIS controllers is calculated as 3.98 % and 4.08 %, respectively. These values meet the requirements of international standards.

The following simulation results are presented to investigate the robustness of the ANFIS and PR controllers and their sensitivity against the variations of the system parameters.

In rectifiers, the input voltage is an external parameter, and the output voltage and input current are determined according to the controller performance. So, to investigate the controller robustness, its performance for possible variations of the input voltage should be simulated. In single phase PWM rectifiers, the amplitude variations of the input voltage have almost no effect on the performance of the converter since in the control system, only its angular frequency is used and changes in the input voltage amplitude will only affect the amplitude of the input current. But the change in the frequency of the input voltage will definitely affect the controller performance especially when the PR controller is employed to regulate the input current. The reason is that the PR controller is designed according to a specific frequency, and any changes in the frequency will reduce the quality of its performance. In this regard, the controller performance has been simulated for different values of grid frequency, the result of which is presented in Table 3.

Table 3. THD value (%) of the input current for grid frequency variations.

f (Hz)	48	48.5	49	49.5	50	50.5	51	51.5	52
PR	5.12	4.67	5.29	5.55	3.98	4.42	4.25	4.19	4.39
ANFIS	4.11	4.11	4.11	4.10	4.08	4.09	4.10	4.09	4.07

As it is obvious in this table, the effects of frequency variations on the performance of ANFIS controller are almost ignorable since, unlike the PR controller, its design is not established based on a specific frequency.

The next simulation results are related to the controllers' performance against harmonic disturbances in the input voltage. In this case, different harmonics have been added to the input voltage, and the performances of the ANFIS and PR controller have been compared in such a situation. Table 4 presents the results of this study in which the amplitude of the 3^{rd}, 5^{th}, 7^{th}, and 9^{th} harmonic is considered 1/10, 1/15, 1/20, and 1/25 of the main component amplitude, respectively. Also, Figures 11 and 12 show the input voltage containing all the mentioned harmonics and its FFT analysis, respectively. About the results presented in Table 4, it should be mentioned that the achieved THD values do not meet international standards as they are higher than 5%. Its reason is that, in this case, exaggerated values are considered for the amplitude of the harmonics to better show the difference between the performance of the

ANFIS and PR controller, and in practice, the amplitude of those harmonics is much lower than the values considered in this test. However, even in such an exaggerated situation, it was possible to achieve lower THD values; for this purpose, a bank of PR controllers synchronized to the harmonic frequencies, called Multi-Resonant controller, could be employed instead of the PR controller used in this work to regulate the input current. This concept is known as harmonic compensation in power electronics (Castilla et al., 2009).

Table 4. THD value (%) of the input current for input voltage with harmonics distortions.

harmonics	-	3	3,5	3,5,7	3,5,7,9
PR	3.98	7.64	8.45	9.24	9.52
ANFIS	4.08	5.86	6.54	7.08	7.45

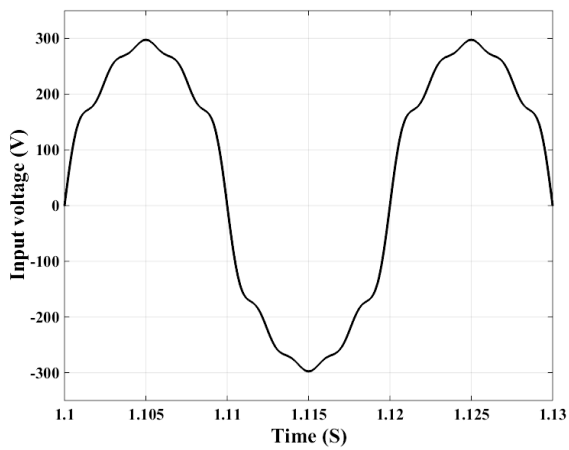

Figure 11. The input voltage containing all the mentioned harmonics.

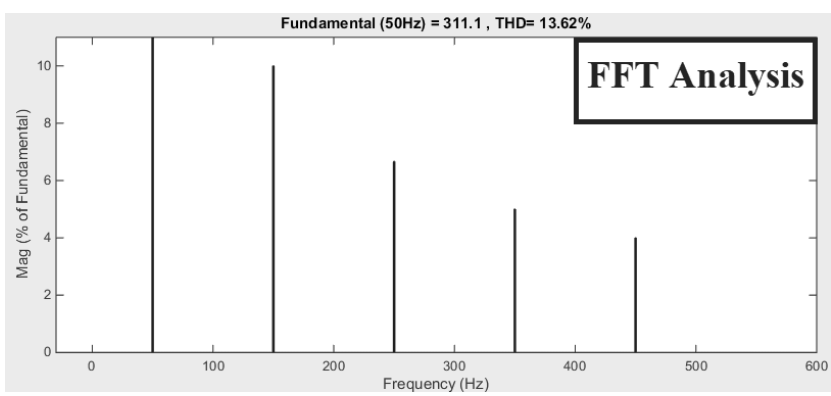

Figure 12. FFT analysis of the input voltage containing all the mentioned harmonics.

Other parameters that can affect the controller performance are the passive elements. The variations of the output filter and load are investigated in the next sub-section, and here, the effect of the variations of the input inductive filter has been studied. Table 5 presents the input current THD value for different values of the input inductor.

Table 5. THD value (%) of the input current for different values of the input filter inductance.

L_1(mH)	3.5	4	4.5	5	5.5	6	6.5	7	7.5
PR	7.37	6.56	5.85	5.33	4.91	4.54	4.35	3.98	3.93
ANFIS	6.98	6.27	5.59	5.12	4.88	4.60	4.39	4.08	3.91

Tables 3-5 clearly confirm the superiority of the proposed ANFIS controller compared to the PR controller, which is employed in the conventional control system of single-phase PWM rectifiers, in terms of robustness and sensitivity against the variations of the system parameters.

Simulation of the rectifier with the power decoupling circuit

After verifying the effectiveness of the proposed ANFIS controller as the current controller in the conventional control system of the rectifier, the efficiency of the proposed methods for decoupling the fluctuating power is studied and the results of the two methods are compared with each other and with those of the method suggested in Li et al. (2013). In the simulation of the proposed methods, a small capacitor (220μF) is used as the output filter, and the auxiliary energy storage element is a 10 mH inductor. The DC-link voltage of the rectifier with fluctuating power elimination using two PR controllers (in part i and part ii of Figure 3) and two ANFIS controllers (in part i and part ii of Figure 3) is illustrated in Fig. 13(a) and Fig. 13(b), respectively.

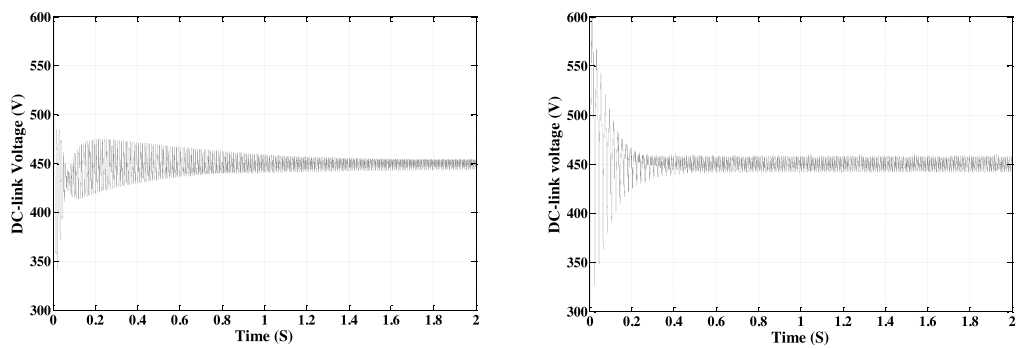

(a) (b)

Figure 13. The DC-link voltage with fluctuating power suppression (a) using two PR controllers (b) using two ANFIS controllers.

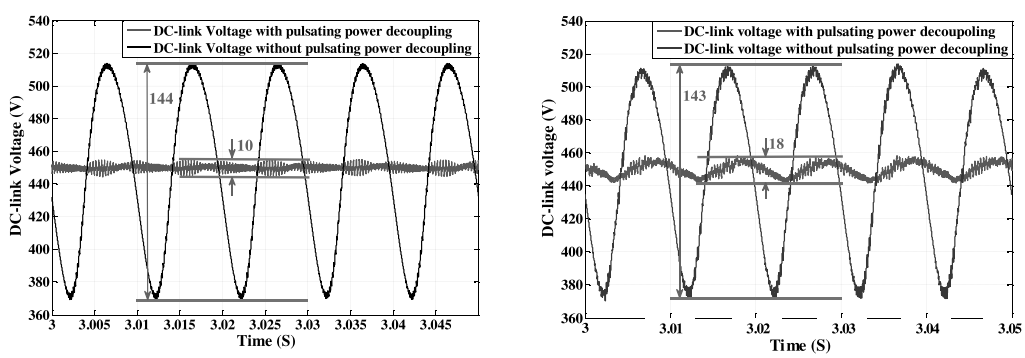

(a) (b)

Figure 14. The DC-link voltage with/without fluctuating power suppression: (a) using two PR controllers; (b) using two ANFIS controllers.

Fig. 14(a) and Fig. 14(b) show the output voltage of the rectifier with/without pulsating power suppression using two PR current controllers or two ANFIS current controllers, respectively. According to the figures, both controllers performed their tasks correctly. The difference is that the ANFIS controller has faster transient than the PR controller. On the other hand, the output voltage ripple using PR controller is lower in the steady state. The lower output voltage ripple arises from the better reference current tracking, which means that the steady state error of the PR controller is less than the ANFIS controller in this case. It should be mentioned that, without fluctuating power filtering to achieve a 10 V output voltage ripple (peak-to-peak), a 2900 μF capacitor, which is more than 13 times larger than the used capacitor, is required at the DC-link. The current THD with fluctuating power decoupling at various times is given in Table 6. It is calculated by analyzing 2 cycles after the mentioned times in Table 6, by using Simulink FFT analysis. Again, the faster transient of ANFIS controller is obvious in Table 6.

Table 6. THD (%) of Input current with power decoupling using PR and ANFIS controllers.

Time (S)	0.1	0.3	0.5	0.7	0.9	1.1	1.3	1.5	1.7	1.9
PR	14.90	11.86	8.86	6.82	5.36	4.45	4.17	4.06	3.97	3.82
ANFIS	14.47	4.33	3.95	4.01	4.13	4.02	4.06	4.08	4.05	4.02

To study the system dynamics while using the suggested methods, the output voltage under step load changes using two PR controllers and two ANFIS controllers is illustrated in Fig. 15(a) and Fig. 15(b), respectively. The load has been decreased 50% suddenly at 3 sec. and increased 100% suddenly at 5.5 sec. Both controllers have a proper performance against the load changes.

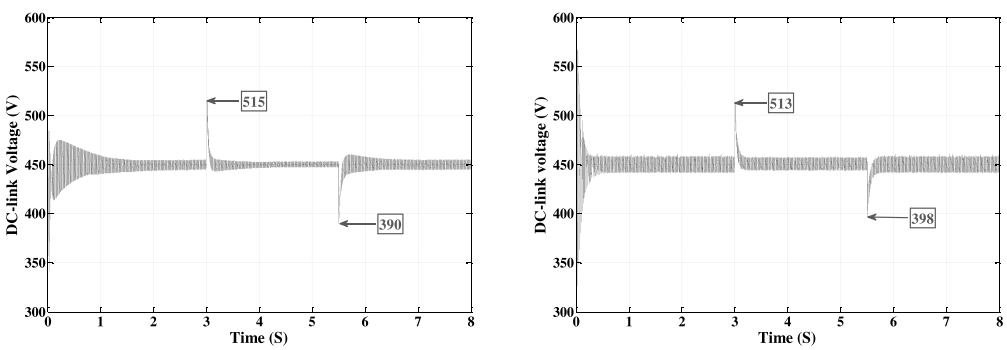

(a) (b)

Figure 15. The DC side voltage changes under the step load variations with power decoupling (a) using two PR controllers (b) using two ANFIS controllers.

Figure 15 demonstrates that, by using two ANFIS controllers, the output voltage changes under the step load variations are less than their changes while using two PR controllers. In addition, the ANFIS controllers have shown a better and faster transient state in this case. Figure 16 indicates the current of the auxiliary inductor (L_f) under the step load variations. For peer review of the controllers' performance, the reference current, actual current, and current error of L_f, exactly at the moment of the load changing have been demonstrated simultaneously in Figure 17. Considering the currents error in Figure 17, it is clear that the ANFIS controller is able to stabilize the current in a negligible time after the load changes and the error value after this change has not only not increased, but also decreased. On the other side, the error value using the PR controller after the load variation has been increased and it requires a short time to reach the steady state. The effect of this point is also clearly visible in Figure 16. These results, once again, confirm the fast transient of the ANFIS controller.

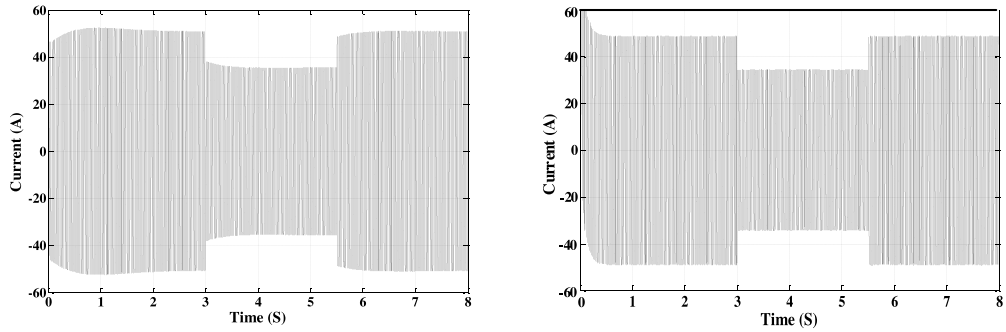

(a) (b)

Figure 16. The auxiliary inductor current under the step load variations: (a) using two PR controllers; (b) using two ANFIS controllers.

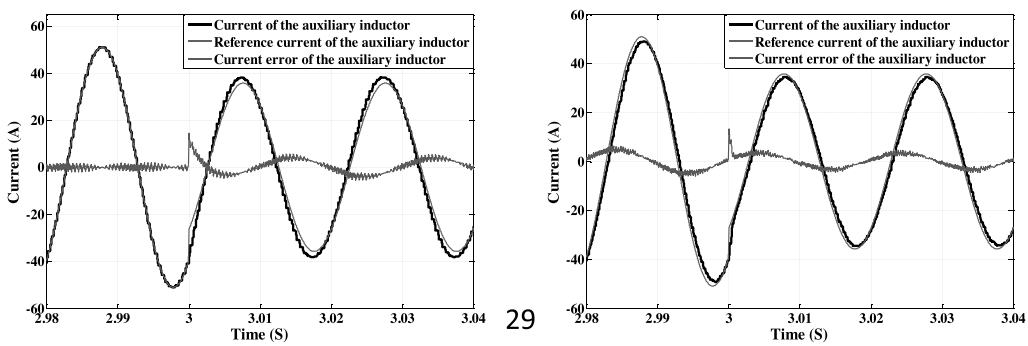

29

(a) (b)

Figure 17. The actual current, reference current, and current error of the auxiliary inductor, at the moment of load changing: (a) using two PR controllers; (b) using two ANFIS controllers.

To validate the performance of the proposed methods, in addition to the fact that the output voltage with/without the fluctuating power suppression has been presented, the simulation results are also compared with the reported simulation results obtained by the method presented in Li et al. (2013), which have studied the same rectifier with the same power rate and almost similar system parameters. The difference between the simulation parameters in our work and that of the mentioned paper is f_{sw} and L_1, which were selected as 2 kHz and 8.5 mH in that work. The smaller inductive input filter used in our work leads to decreasing the volume and cost of the converter. The results obtained by our proposed methods and the method suggested in Li et al. (2013) are given in Table 7. The 100-Hz component in the DC-link voltage (V) is calculated using FFT analysis from t=1.5 sec. to t=3 sec. (150cycles). It is worth mentioning that the proposed topology in Li et al. (2013) uses a 220 μF capacitor as the auxiliary energy storage element that has lower volume and higher power density in comparison to the auxiliary inductor used in this paper. However, the proposed method in this work has several advantages compared to that of Li et al. (2013) and other previous methods as follows:

1) More reliability and robustness due to the use of inductor as the auxiliary energy storage element,

2) Less complexity in the control method that makes its implementation simpler,

3) Faster transient, more robustness, and less sensitivity against possible variations in system conditions, using the ANFIS controller because of its online learning ability that leads to a high adaption capability of the control system.

Table 7. The results obtained in the simulation of the proposed methods and the simulation results reported in Li et al. (2013).

	Output voltage ripple of the rectifier (V)	100-Hz component in DC-link voltage (V)
Without pulsating power decoupling in (Li et al., 2013)	130	60.24
Without pulsating power decoupling using PR controller	144	68.33
Without pulsating power decoupling using ANFIS controller	143	66.01
With pulsating power decoupling in (Li et al., 2013) without reference modification	20	7.99
With pulsating power decoupling in (Li et al., 2013) with reference modification	9	0.15
With pulsating power decoupling using PR controllers	10	0.34
With pulsating power decoupling using ANFIS controllers	18	5.376

CONCLUSION

This paper presented an active filtering method for eliminating the input pulsating power of single-phase PWM rectifiers, in which the concept and basic structure of the proposed control system are simpler than those of other existing methods. For the suggested control system, two current controllers with different types based on PR and ANFIS structures are proposed. The effectiveness of both methods in pulsating power elimination is verified by system simulation in various conditions. Each of the proposed controllers has its specific advantages. The PR controller showed an acceptable transient and a small steady-state error in tracking the sinusoidal reference that leads to a suitable performance in the fluctuating power suppression. The ANFIS controller provided an acceptable steady state error and showed a very fast transient and robustness against the possible variations in the system condition due to its online learning ability that makes it highly adaptable to different situations. In addition, this paper proposed a superseded control technique based on the ANFIS architecture for the conventional control system of the single phase PWM rectifier. The simulation results demonstrated that the ANFIS controller is able to stabilize the output voltage and obtain a grid current with low distortion and the unity power factor operation as well as the conventional control method. Its advantages over the conventional method are providing better and faster transient and showing less sensitivity and more robustness against the variations of the system parameters due to its capabilities.

REFERENCES

Castilla, M., Miret, J., Matas, J., de Vicuña, L.G. & Guerrero, J.M. 2009. Control design guidelines for single-phase grid-connected photovoltaic inverters with damped resonant harmonic compensators. IEEE Transactions on industrial electronics, **56**(11):4492-4501.

Li, H., Zhang, K., Zhao, H., Fan, S. & Xiong, J. 2013. Active power decoupling for high-power single-phase PWM rectifiers. IEEE Transactions on Power Electronics, **28**(3):1308-1319.

Liu, Y.J. & Tong, S. 2015. Adaptive fuzzy control for a class of unknown nonlinear dynamical systems. Fuzzy Sets and Systems, **263**:49-70.

Masood, M.K., Hew, W.P. & Rahim, N.A. 2012. Review of ANFIS-based control of induction motors. Journal of Intelligent & Fuzzy Systems, **23**(4):143-158.

Mohan, N. & Undeland, T.M. 2007. Power electronics: converters, applications, and design. John Wiley & Sons.

Qi, W., Wang, H., Tan, X., Wang, G. & Ngo, K.D. 2014. A novel active power decoupling single-phase PWM rectifier topology. In Applied Power Electronics Conference and Exposition (APEC), 2014 Twenty-Ninth Annual IEEE, pp:89-95.

Rezaei, H., Rastegar, H. & Pichan, M. 2015. A new active power decoupling method for single phase PWM rectifiers. In Iranian Conference on Electrical Engineering (ICEE), 2015 23rd Annual IEEE, pp. 1665-1670.

Rezaie, H., Rastegar, H. & Pichan, M. 2016. Reduced size single-phase PHEV charger with output second-order voltage harmonic elimination capability. In Power Electronics and Drive Systems Technologies Conference (PEDSTC), 2016 7th Annual IEEE, pp. 492-497.

Rezaie, H., Moosavy Chashmi, S.M., Mirsalim, M. & Rastegar, H. 2017. Enhancing LVRT Capability and Smoothing Power Fluctuations of a DFIG-based Wind Farm in a DC Microgrid. Electric Power Components and Systems, **45**(10):1080-1090.

Shimizu, T., Fujita, T., Kimura, G. & Hirose, J. 1997. A unity power factor PWM rectifier with DC ripple compensation. IEEE Transactions on industrial electronics, **44**(4):447-455.

Shimizu, T., Jin, Y. & Kimura, G. 2000. DC ripple current reduction on a single-phase PWM voltage source rectifier. IEEE Transactions on Industry Applications, **36**(5):1419–1429.

Su, M., Pan, P., Long, X., Sun, Y. & Yang, J. 2014. An active power-decoupling method for single-phase AC–DC converters. IEEE Transactions on Industrial Informatics, **10**(1):461-468.

Tang, Y. & Blaabjerg, F. 2015. A component-minimized single-phase active power decoupling circuit with reduced current stress to semiconductor switches. IEEE Transactions on Power Electronics, **30**(6):2905-2910.

Tang, Y., Blaabjerg, F., Loh, P.C., Jin, C. & Wang, P. 2015. Decoupling of fluctuating power in single-phase systems through a symmetrical half-bridge circuit. IEEE Transactions on Power Electronics, **30**(4):1855-1865.

Tripura, P. & Babu, Y. 2014. Intelligent speed control of DC motor using ANFIS. Journal of Intelligent & Fuzzy Systems, **26**(1):223-227.

Wang, R., Wang, F., Boroyevich, D., Burgos, R., Lai, R., Ning, P. & Rajashekara, K. 2011. A high power density single-phase PWM rectifier with active ripple energy storage. IEEE Transactions on Power Electronics, **26**(5):1430-1443.

Yazdani, A. & Iravani, R. 2010. Voltage-sourced converters in power systems: modeling, control, and applications. John Wiley & Sons.

Zammit, D., Staines, C.S. & Apap, M. 2014. Comparison between PI and PR current controllers in grid connected PV inverters. WASET, International Journal of Electrical, Electronic Science and Engineering, **8**(2).

Zhang, N., Tang, H. & Yao, C. 2014. A systematic method for designing a PR controller and active damping of the LCL filter for single-phase grid-connected PV inverters. Energies, **7**(6):3934-3954.

Zhong, Q.C., Ming, W.L., Cao, X. & Krstic, M. 2012. Reduction of DC-bus voltage ripples and capacitors for single-phase PWM-controlled rectifiers. In IECON 2012-38th Annual Conference on IEEE Industrial Electronics Society, pp:708-713.

Submitted: 10/10/2017
Revised: 14/09/2018
Accepted: 11/11/2018

طريقة جديدة لفصل الطاقة المتقلبة ترتكز على هياكل التحكم ANFIS و PR القابلة للتطبيق على مقومات PWM أحادية الطور

حميد رضائی، علی رضا خوش سعادت، جواد شکراللهی مغانی وحسن رستکار
قسم الهندسة الكهربائية، جامعة أميركبير الصناعية، طهران، إيران
قسم الهندسة الكهربائية، جامعة آية الله بروجردی، بروجرد، ايران

الخلاصة

في مدخلات الطاقة لمقومات أحادية الطور يوجد جزء نابض مع شبكة تواتر. لمنع انتقال الطاقة النابضة إلى قسم التيار المستمر، يجب أن يتم تصفيتها جيداً وبطريقة مناسبة. لهذا الغرض، تتمثل الطريقة المناسبة في تثبيت مكثف عالي السعة في قسم التيار المستمر، والذي لا يمكن اعتباره حلاً مناسباً بسبب خصائصه غير المرغوب فيها. يقترح هذا البحث طريقة فعالة للتخلص من الطاقة النابضة، والذي فيها يعتمد جهاز التحكم على هيكل نظام الاستدلال الضبابي القائم على شبكة التكيف (ANFIS). ولتحسين أداء وحدة التحكم، تم استخدام خوارزمية تعلم عبر الإنترنت ترتكز على طريقة الانتشار الخلفي للخطأ (EBP). تؤدي هذه التقنية إلى تشكيل نظام تحكم مع بنية مصغرة محسنة من حيث الدقة، ومطورة ديناميكياً. تم كذلك تطبيق استراتيجية التحكم المقترحة باستخدام رنين نسبي (PR)، وتم مقارنة أداء النظامين مع بعضهما البعض ومع واحد من أفضل الأعمال السابقة. علاوة على ذلك، تم اقتراح طريقة تحكم مبنية على ANFIS لنظام التحكم التقليدي لمقومات PWM أحادية الطور. تم تأكيد كفاءة الطرق المقترحة من خلال عمليات محاكاة واسعة النطاق في MATLAB / Simulink.